

Konstantin V. Savelkin
Dmitry A. Yarantsev

(Joint Institute for High Temperatures, Russian Academy of Sciences, 125412 Moscow, Russia)

Sergey B. Leonov

(Joint Institute for High Temperatures, Russian Academy of Sciences, 125412 Moscow, Russia)
 (Department of Aerospace and Mechanical Engineering, University of Notre Dame, Notre Dame, IN, 46556, USA)

E-mail : leonov.1@nd.edu

DOI: 10.12762/2015.AL10-08

Experiments on Plasma-Assisted Combustion in a Supersonic Flow: Optimization of Plasma Position in Relation to the Fuel Injector

The results of an experimental study of plasma-induced ethylene ignition and flameholding in a supersonic model combustor are presented in the paper. The experimental combustor has a cross-section of 72 mm (width) x 60 mm (height) and length of 600 mm. The fuel is directly injected into the supersonic airflow through wall orifices. The flow parameters are: Mach number $M=2$, static pressure $P_{st}=160-250$ Torr, stagnation temperature $T_0=300$ K and total air flow rate $G_{air} \leq 0.9$ kg/s. The near-surface quasi-DC electrical discharge is generated by a series of flush-mounted electrodes, providing an electrical power deposition of $W_{pl}=3-24$ kW. The scope of the experiments includes the characterization of the discharge interacting with the main flow and fuel injection jet, a parametric study of ignition and flame front dynamics and a comparison of three plasma generation schemes: the first two examine upstream and downstream locations of plasma generators in relation to the fuel injectors. The third pattern follows a novel approach of a combined mixing/ignition technique, where the electrical discharge is distributed along the fuel jet, starting within the fuel injector. The last pattern demonstrates a significant advantage in terms of the flameholding limit. The experiments are supported by gas temperature and H_2O vapor concentration measurements by Tunable Diode-Laser Absorption Spectroscopy (TDLAS). The technique studied in this work has weighty potential for high-speed combustion applications, including cold start/restart of scramjet engines and support of the transition regime in a dual-mode scramjet and during off-design operation.

Introduction

Ignition and stabilization of combustion in supersonic flows at low and moderate entry total enthalpies is a problem of major fundamental and applied importance in the development of hypersonic vehicles. The use of gaseous plasma generated in electrical discharges for the stabilization of supersonic combustion is one of the most promising approaches. Compared to a basic scramjet layout, the scheme with plasma assistance delivers more freedom in the choice of the geometric configuration, due to the replacement of a mechanical flameholder with a highly effective electrically driven apparatus. Prospectively, the use of this method could lead to a reduction in total pressure losses under non-optimal conditions, to the enhancement of operation stability and, consequently, to expanding the limitations in scramjet operability.

The concept of Plasma-Induced Ignition and Plasma-Assisted Combustion is considered on the basis of three main ideas: the gas heating/non-equilibrium excitation by the discharge, fuel-air mixing in-

tensification and flow structure control in the vicinity of the reaction zone. Over the years, many studies have been conducted to develop an alternative plasma-based ignition system that could consistently and reliably ignite non-stoichiometric mixtures at a wide range of pressures and temperatures [1-3]. Most plasma technologies rely on a high energy density electrical discharge to ionize the mixture and initiate combustion due to a thermal/chemical activation of the fuel or air/fuel mixture [3-5]. Likewise, the experimental studies were performed under conditions that are typical for scramjet operation [6-10]. A basic geometric configuration was used for the duct, which includes a backward wallstep or contoured cavity. Factually, plasma is used as an igniter of a combustible mixture in a low-speed zone. At the same time, previous experiments with this configuration, where an electric discharge is used with a plane wall arrangement [11-12], demonstrate the feasibility of plasma application as an effective igniter, mixer and flameholder in a supersonic combustor without the help of any mechanical obstacles.

Another pole of the problem is highly non-equilibrium chemical kinetics, which may help to reduce plasma power for the fuel-oxidizer mixture ignition, due to variable selectivity of chemical reaction pathways. Significant progress in this domain over the last 15 years is apparent [3-5, 13-15]. It has been shown that a dramatic reduction in the ignition time up to orders of magnitude occurs at premixed conditions, including a range of gas temperatures that is specifically important for scramjet technology, $T_o=500-900\text{ K}$. Despite being very promising, such an approach seems to be of little practicality for high-speed engines with direct fuel injection. Under most conditions, the main limiting factor is rather slow mixing, resulting in a strong fuel/oxidizer ratio gradient across the combustion chamber. The most challenging issue in this case is the proper location of a typically non-uniform discharge in a shear layer between the fuel jet and the surrounding airflow.

A novel pattern of plasma-fuel interaction is examined in this paper and is compared to previously tested configurations, where plasma is generated in the air in front of the fuel injection [11-12, 16]. In the current scheme, electric discharge is partially located inside of an injection orifice, chemically pre-processing the fuel and accelerating the mixing due to the introduction of strong thermal inhomogeneity into the flow field. The idea exploits the effect of discharge specific localization in the shear layer with a gradient concentration of two gases [17]. For future research, such an approach appears to be quite prospective to promote mixing and flameholding in a supersonic combustor.

Experimental apparatus and diagnostics

The experiments were performed in a supersonic blow-down wind tunnel PWT-50H [11 12], the schematic drawing of which is shown in figure 1. In this configuration, the test section operates as a supersonic combustor, with the fuel injectors and electrical discharge generator flush-mounted on a plane wall [18], as shown tentatively in figure 1b. The combustor cross-section is $Y \times Z = 72\text{ mm}$ (width) $\times 60\text{ mm}$ (height), with a length of $X = 600\text{ mm}$. In order to avoid thermal choking during fuel ignition, the test section has a 10° expansion angle downstream of the injectors on the opposite (bottom) wall to the cross-section of $Y \times Z = 72\text{ mm} \times 72\text{ mm}$. The experimental conditions are as follows: initial Mach number $M=2$; static pressure $P_{st}=160-250\text{ Torr}$; air mass flow rate $G_{air}=0.6-0.9\text{ kg/s}$; fuel (ethylene) mass flow rate $G_{C_2H_4}=1-8\text{ g/s}$; duration of steady-state aerodynamic operation $t \leq 0.5\text{ s}$. The PWT-50H high-speed combustion facility test section is equipped with 3 pairs of 100 mm diameter windows placed in the side walls of the duct for optical access. The first pair of windows is located near the upstream side of the combustor and provides optical access to the plasma-fuel-flow interaction area. The second pair of windows is placed downstream, with a 65 mm gap between the two pairs of windows. The third pair of windows is typically used for TDLAS measurements, as has been done in our previous work [16]. Instrumentation includes the pressure measuring system, the schlieren system, a UV/visible optical emission spectrometer, current and voltage sensors, a Tunable Diode Laser Absorption Spectroscopy (TDLAS) apparatus for water vapor temperature/concentration measurements, a 5-component exhaust flow chemical analyzer, high-speed cameras and operation sensors.

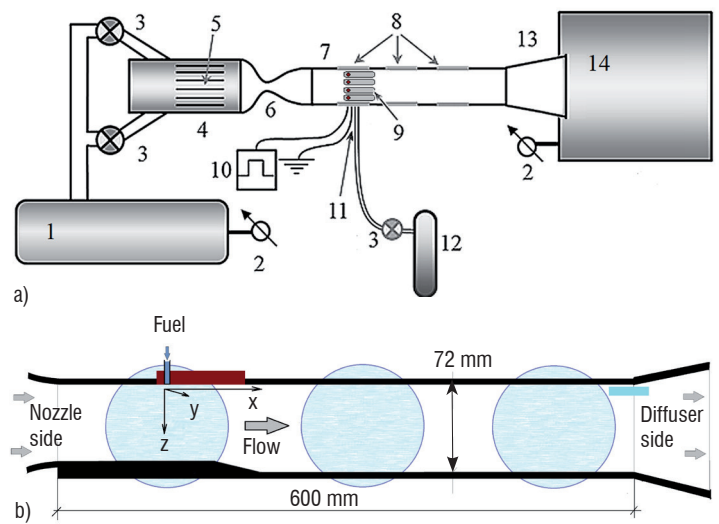


Figure 1 - Schematic drawing of the PWT-50H experimental facility.
a) General layout : 1- high pressure tank ; 2 - operation gauges ; 3 - solenoid valves ; 4 - plenum section ; 5 - honeycomb ; 6 - nozzle ; 7 - test section ; 8 - optical access windows ; 9 - plasma-injector modules ; 10 - high-voltage power supply ; 11 - fuel ports / discharge connectors ; 12 - fuel tank ; 13 - diffuser ; 14 - low-pressure tank.
b) Test section wall profile : optical windows are indicated by circles, the location of the plasma-injector modules is shown by a rectangle in the top wall of the test section.

Three basic schemes were examined for the injectors and plasma generator arrangement, as shown in figure 2.

Scheme N° 1

Electrodes located upstream of the fuel injectors. Plasma is generated mostly in air and then interacts with the injected fuel [12].

Scheme N° 2

Electrodes located downstream from the fuel injectors. An electrical discharge is generated in non-uniform air-fuel composition [16].

Scheme N° 3

The electrical discharge collocates with the fuel jet [24].

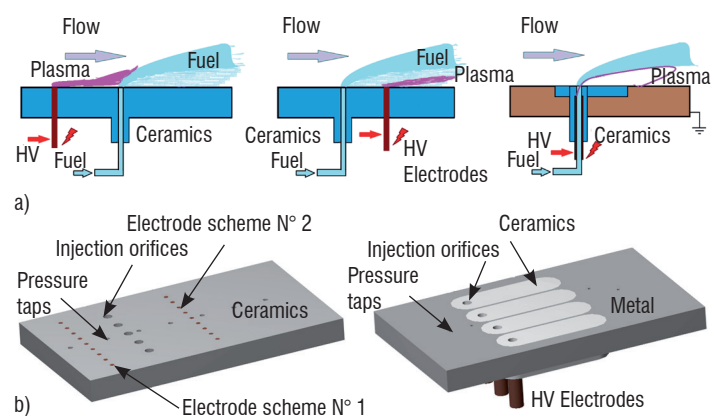


Figure 2 - Schematic drawing of three basic layouts for the fuel injectors and electrode arrangement.

- a) : 3D view of two insertions used during testing.
b) : the left image is for Scheme N° 1 and Scheme N° 2 ; the right image is for Scheme N° 3.

In the first two patterns, the fuel is injected through 5 circular ($d=3.5$ mm) orifices all in a row across the span, as shown in figure 2b. The row of injectors is located at 20 mm downstream from the first row of electrodes and 30 mm upstream from the second one. The fuel mass flow rate was balanced between the orifices using a fuel plenum. The duration of the discharge was in the range 70-120 ms; typically it was 100 ms. Fuel injection was started 20 ms after the discharge initiation. Usually, the fuel injection continued for 10-20 ms after the discharge, in order to observe whether the flame was held or extinguished. The injection could be organized downstream or upstream from the discharge zone by switching between two rows of electrodes. For the third scheme, four injection-ignition modules (PIM) were installed in the combustor with the same fuel injection and plasma operation time diagram. The high-voltage electrode (anode) is integrated into the fuel injector. For this, a metal tube is inserted into a ceramic injection orifice. The distance between the end of the tube and the duct wall surface, $ZI \leq 10$ mm, is long enough to ensure significant impact of the discharge on the fuel flow prior to its injection into the main airflow.

The custom-made power supply used in these experiments is designed to operate with a steep falling voltage-current characteristic and individual control of each output channel. Control of output power is performed by varying the internal resistance of the power supply. Under typical experimental conditions, the power supply operates in nearly current-stabilized mode. Voltage across the gap and discharge current are measured using a Tektronix P6015A high-voltage probe and Agilent 1146A current probe during the run for each module, which enables the discharge power coupled to the individual PIM to be calculated.

The facility is equipped with a NetScanner 9116 static pressure scanner with 16 static pressure sensors, B1 - B16, a stagnation pressure sensor $P_{P_{tot}}$, and a pressure in vacuum tank sensor P_{ip} . Schlieren visualization was used as the main tool to study the dynamics of the flow structure modification during fuel ignition induced by the plasma. The high-resolution schlieren system uses a high-power pulsed diode laser (pulse duration $t_{exp} = 100$ ns) and a framing camera (frame rate of up to 1000 frames per second, Basler A504K). The plasma luminescence emission spectra were recorded by the Lot-ORIEL spectrometer with an Andor CCD camera. The spectral dispersion is 0.035 nm/pixel and the spectral resolution is $\Delta\lambda = 0.13$ nm. The spectroscopic system collects plasma emissions from a cylindrical volume with a diameter of 10 mm aligned in the Y direction from window to window. During the operation, the spectrometer records an emission spectrum every 10 ms.

Near-surface quasi-DC electrical discharge characterization in a high-speed flow

Typical photographs of the discharge appearance, taken during operation in Scheme N°.1 and Scheme N°.3, without and with fuel injection, are presented in figure 3. In Scheme N°.2 the discharge without injection looks very similar to Scheme N°.1. Hydrocarbon fuel injection leads to a significant increase in the discharge luminescence in the interaction zones, mostly due to strong CN and C2 molecular band amplification. The total discharge power in all cases was $W_{pl} = 6-24$ kW. Both the discharge voltage and current were oscillating because of discharge filament length variations, within a range

of $U_{pl} = 0.7-2$ kV and $I_{pl} = 2-7$ A, respectively. Prior to fuel injection, the discharge power was distributed equally between the electrodes.

Characterizing the discharge parameters and dynamics, the description below is focused on Scheme N°. 3. The detailed data for the discharge in Modes N°.1 and N°.2 are presented in the publications [12, 16, 18]. At the beginning of the plasma filament development, a breakdown occurs along the path inside the injector and a short gap between the injection orifice and a grounded metal wall upstream from the injector. After this, the filaments are convected by the flow downstream from the injector, ending at the grounded wall downstream from the ceramic inserts, shown in figure 2. After this occurs, the plasma filaments extend downstream over a distance of up to 100 mm, close to the surface of the ceramic insert. The location of the filament ends at the grounded wall oscillates at a frequency of $F = 10-20$ kHz. The filament behavior changes significantly after fuel injection. Specifically, plasma emission intensity increases and the plasma filaments move away from the surface

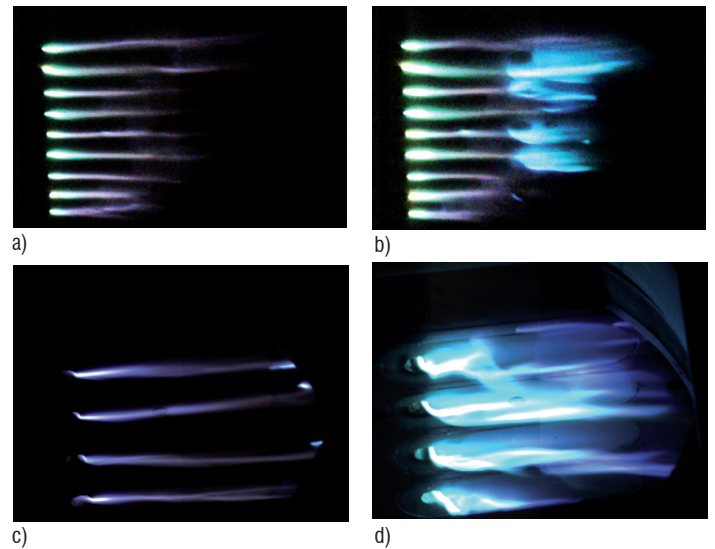


Figure 3 - Photographs of an electrical discharge in the combustion chamber, with an exposure time of $t = 100$ μ s (compare to figure 2b for details). Scheme N°.1: (a) no ethylene injection ; (b) ethylene injection enabled. Scheme N°.3: (c) no ethylene injection ; (d) ethylene injection enabled.

The typical dynamics of time-resolved discharge power for 4 individual modules is shown in figure 4(a). Despite the large magnitude of the high-frequency oscillations, the time-averaged power values are quite stable and repeatable from run to run. It is also seen that the value of the discharge power varies during the run. Fuel injection and ignition lead to an increase in the discharge power in the central modules, due to a significant extension of the length of plasma filaments and the resultant rise of gap voltage, as shown in figure 4(b). At a certain value of the fuel injection flow rate, the intense heat release in chemical reactions in the near-centerline zone of the combustor induces flow separation near the duct corners, which consequently reduces the length of the lateral plasma filaments, as well as the discharge power in the lateral modules. The discharge power can be regulated by varying the average output current of the power supply. It should be noted that the power deposition is not proportional to the average discharge current, because increasing the current somewhat reduces the gap voltage. The operation characteristics of individual PIM modules depend to some extent on whether the adjacent modules are powered or not, especially for the lateral modules.

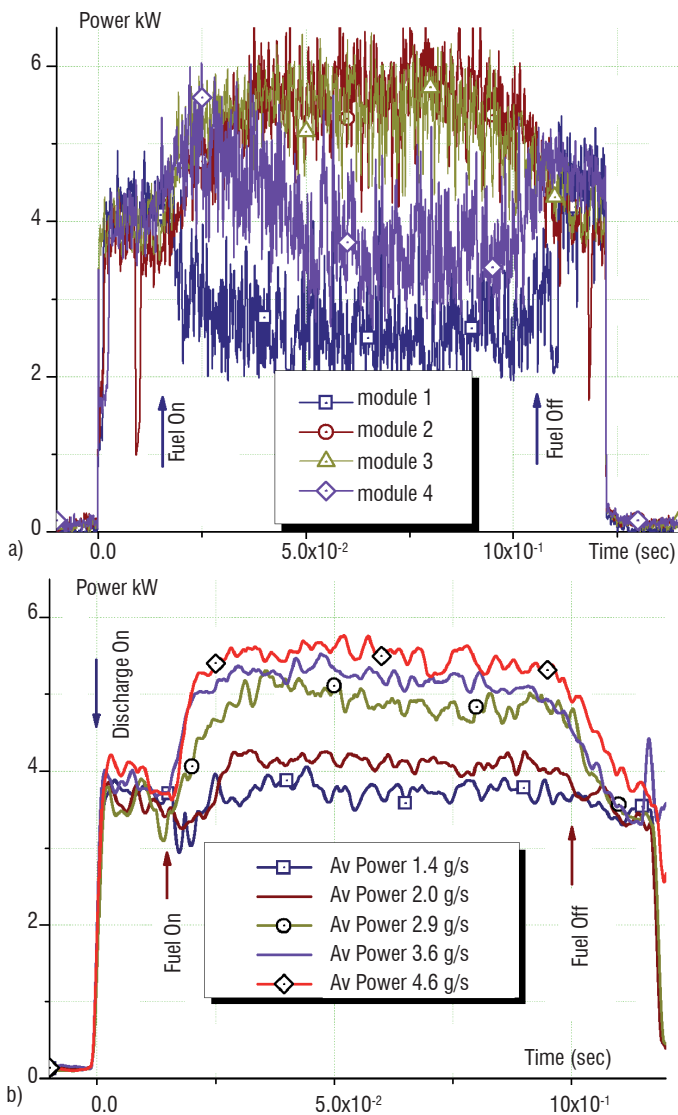


Figure 4 - (a) Discharge power dynamics and distribution among the PIM modules, calculated from voltage and current measurements. $G_{C_2H_4}=3$ g/s ; averaged current $I_{pl}=4A$. (b) Discharge power in Module N° 3 vs. fuel injection flow rate. A low-pass filter is applied to reduce high-frequency oscillations.

A composite optical emission spectrum of the plasma, obtained by integrating the emission from the plasma-fuel-flow interaction area, $x=20-30mm$, $y=0-10$ mm, is shown in figure 5. Analysis of the spectra shows that, in the presence of the hydrocarbon fuel, three different types of species are detected: hydrocarbon/carbon fragments, chemical reaction products resulting from the interaction of hydrocarbon plasma and air, and excited air species (mainly N_2). The species with the highest emission intensity include atomic hydrogen, carbon and oxygen (O atom triplet line at $\lambda=777$ nm outside of the spectral range of figure 5), hydrogen molecule H_2 , as well as C_2 , CN , OH and CH radicals. Neglecting continuum emission, the molecular bands of the CN radical violet system, $CN(B^2\Sigma \rightarrow X^2\Sigma)$ and C_2 Swan bands contribute up to 50% of the integrated emission intensity. These spectra indicate intense chemical transformations in the flow, including the generation of active radicals in electronically excited states. The emission spectra were used to evaluate plasma parameters in a zone near the base of the fuel injection jet. A second positive system of molecular nitrogen, $N_2(C^3\Pi_u, v'=0 \rightarrow B^3\Pi_g, v''=0)$ band at $\lambda=337.1$ nm, was used to infer the rotational-translational temperature in the plasma [19], $T_r=3000 \pm 500$ K, which is strongly weighted toward

the peak temperature in the plasma filament. The H atom Balmer series lines are very intense, with the H_α line at $\lambda=656.3$ nm being the strongest in this case. Electron density in the plasma was extracted from the H_α spectral line shape [20, 21], since the Stark effect is the dominant mechanism of line broadening under these conditions. Electron density near the base of the fuel injection jet is inferred to be $n_e=(4.51.0)10^{15}$ cm⁻³.

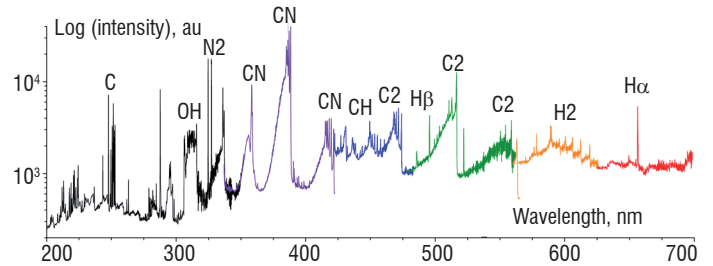


Figure 5 - Survey optical emission spectrum obtained from the ethylene-air-flow-plasma interaction region. The spectrum incorporates seven overlapping spectra, obtained separately under the same conditions. Discharge current $I_{pl}=2-4A$, ethylene injection jet $G_{C_2H_4}=0.5-1$ g/s from each module in $M=2$ airflow, $P_{st}=180-220$ Torr. Major emission lines and bands are labeled.

The mechanism of plasma interaction with a jet of fuel injected into the airflow is of major importance for the dynamics of ignition and flameholding under these conditions. From a comparison of the images in figure 3c and figure 3d, it is apparent that plasma emission, which serves as an indicator of energy loading by the discharge (i.e., indicating the presence of both an electric field and discharge current), essentially follows the fuel jet. The effect of the electrical current convecting with the flow has been previously observed in a near-surface transverse filament discharge between two pin electrodes in Mach 2 airflow [18, 22]. In Mach 2.8 airflow, a near-surface transverse DC discharge filament between two electrodes extended in the flow direction convected in the boundary layer at a velocity of approximately 60% of the free stream velocity [23]. A quantitative prediction of the discharge behavior in the fuel injection flow under these conditions can be obtained using a plasma fluid model, incorporating equations for electron and ion densities and the Poisson equation for the electric field, as discussed in detail in [24]. Quantitatively, the filament shape and discharge current path through the fuel injection jet, reacting mixing layer and the air flow is controlled by the trade-off between at least two factors, (i) the maximum value of the effective ionization coefficient, i.e., the difference between the ionization and attachment coefficients, $\alpha(E/N) - \eta(E/N)$, and (ii) the maximum effect of convection by the flow.

Experimental results on Plasma-assisted combustion : effect of fuel mass flow rate and discharge power

Figure 6 presents typical data for the wall pressure distribution in the case of Schemes N° 1 and N° 2, when the electrode system and fuel injectors are not combined into a single module. The discharge generation without fuel injection slightly affects the pressure distribution, increasing the pressure in the immediate vicinity of the electrode system. When the fuel injection is turned on, the pressure increases slightly in the zone close (downstream) to the injector for the first scheme and close to the plasma area for the second scheme. This increase is associated with the fast reactions of fuel partial oxidation by atomic oxygen O . Other reaction branches are related to

electronically / vibrationally excited nitrogen (N_2^*) and other active species generated in air plasma. In the case of a second scheme, highly reactive species and radicals, such as H , CH and C_2H_3 are involved in the initial fast chemical processes as well. The products of these fast plasma-chemical reactions are accumulated in the associated separation bubble and then are blown down by a core flow. The main chemical power release occurs after fuel mixing with core air in the second combustion stage [11], rather than downstream from the place of plasma generation. In figure 6, this zone is located at $x > 120$ mm. The schlieren image in figure 7a depicts this zone very well ; it is labeled as the "Flame front". At low plasma power $W_{pl} < 8$ kW, the second combustion stage may not be carried out at all. Two effects are responsible for this : (a) insufficient fuel activation by the discharge and (b) insufficient fuel-air mixing enhanced by the plasma. Numerical modeling [25], including plasma-chemical kinetics and mixing processes, indicates that the second effect may be dominant.

Under "optimal" conditions for Scheme N° 2, the zone of intensive chemical reactions moves upstream and stabilizes near the plasma location. This regime is seen in figure 6 for an ethylene mass flow rate $G_{C_2H_4} = 2.1$ g/s . When the flame front is stabilized (during steady-state flameholding), the combustion process appears to progress slowly in the axial direction, due to gradual mixing of fuel and air. The chemical energy release during combustion elevates the pressure and forms a wedge-shape combustion zone, with its average angle increasing as combustion intensifies. The associated oblique shock wave angle increases accordingly. It should be noted that this zone is observed during operation in Scheme N° 1 as well; however, the electrical power has to be rather high for this effect to appear, $W_{pl} > 20$ kW. If $G_{C_2H_4} > 3$ g/s, the zone of high energy release moves downwards gradually.

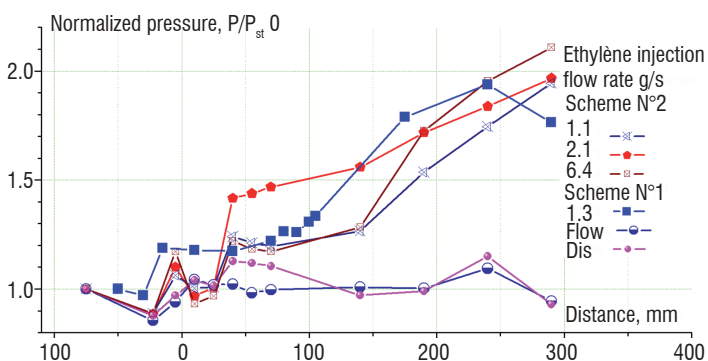


Figure 6 - Normalized wall pressure P/P_{st} distribution during plasma-assisted combustion for Scheme N° 1 and Scheme N° 2. Total discharge power $W_{pl} = 9-12$ kW. The caption numbers indicate an ethylene mass flow rate $G_{C_2H_4}$ in g/s; points labeled "Flow" were obtained without fuel injection, with the discharge turned off; points labeled "Dis" were obtained without fuel injection, with the discharge turned on.

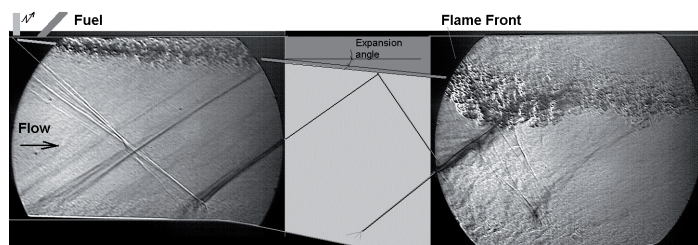
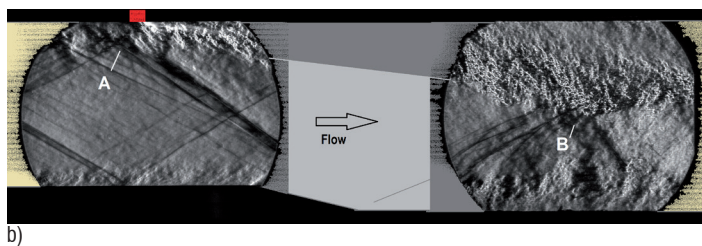


Figure 7 - Composite schlieren image illustrating the flow structure in the test section. It consists of a pair of images taken through two different windows during different runs, combined into one. Black areas show the contour of combustor walls; the electrode positions and point of fuel injection are indicated. The extent of the wedge-like combustion zone between the two windows is interpolated in gray. (a) Scheme N° 1 : ethylene injection mass flow rate $G_{C_2H_4} = 1.3$ g/s. (b) Scheme N° 3 : ethylene injection mass flow rate $G_{C_2H_4} = 3$ g/s.

A series of experiments was performed on ethylene ignition and flameholding by means of the electrical discharge collocated to the fuel injection jet, described above as Scheme N° 3. The following test parameters have been varied : (1) fuel injection flow rate, within a range of $G_{C_2H_4} = 1 - 8$ g/s ; and (2) discharge time-averaged current (i.e., discharge power). First of all, it has been determined that ignition and flameholding are observed over a much wider range of parameters compared to the previously tested configurations for Schemes N° 1 and N° 2, with the electric discharge located both upstream and downstream from the fuel injection port.

Typical schlieren images for Scheme N° 3 are shown in figure 7(b), illustrating the flow structure during combustion. When the discharge is enabled, the location of the plasma filament near the injection orifice becomes visible due to oblique shock generation. The oblique shock wave interacts with an expansion wave generated by angle step expansion of the bottom test section wall (see figure 7b) and then with a compression wave generated there when the flow velocity vector is reversed. Flow separation near the side wall at the PIM location is also evident. A further increase in the fuel mass flow rate would result in the separation zone moving upstream, thus increasing the oblique shock wave angle and eventually leading to thermal choking of the duct.

The other side of the electrical discharge effect on combustion is the enhancement of air-fuel mixing in high-speed flows. Both direct and indirect plasma-flow interaction mechanisms are responsible for this effect. First, plasma-based heating generated in the flow acts as a "gradual" obstacle, generating a vortex flow similar to a Karman vortex trail. An additional, direct, plasma effect is caused by strong modulation of the power deposition in the electric discharge, which results, depending on the discharge location, in boundary or shear layer tripping. As seen in figure 4a, the instantaneous discharge power modulation is up to $\sim 50\%$ of the average power value; the frequency of the modulation is 10-20 kHz. An indirect mixing enhancement mechanism is carried out through the Richtmyer-Meshkov instability, appearing in flows with non-collinear density and pressure gradients. This leads to the formation of deterministic vortex-dominated and, subsequently, small-scale stochastic perturbations resulting in turbulent mixing [25-26]. Two regions of the flow field, labeled as A and B in figure 7b, are of particular interest. In region A, shock waves caused by the test section wall imperfections and originating upstream from the field of view interact with the fuel jet with a high density gradient, caused by plasma-induced non-uniform heating. In region B, the shock wave is caused by the wall wedge and is amplified by a strong shock coming from the PIMs. At the beginning of the PIM operation, this shock impacts the heated near-wall fuel jets, thus enhancing the mixing processes.



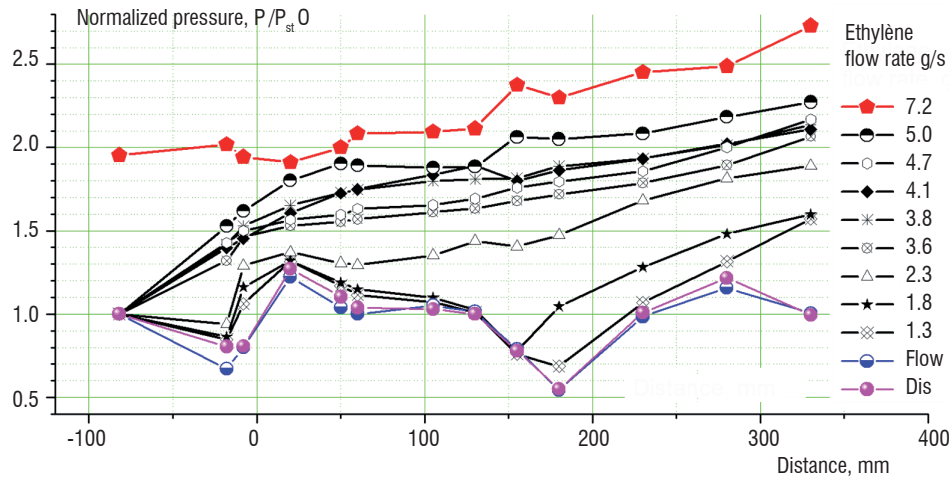


Figure 8 - Normalized pressure $P/P_{st,0}$ profiles along the combustor vs. fuel mass flow rate : Scheme N°. 3, total discharge power $W_{pl} = 16-18 kW$. Compare to figure 6 for Schemes N°. 1 and N°. 2.

In figure 8, pressure distributions measured along the test section are plotted vs. the fuel mass flow rate. At high enough values of the discharge power and fuel injection mass flow rate, a significant increase is observed in the wall pressure over a wide range of fuel flow rates. In lean mixtures, ignition is detected downstream, as far as $x > 250 mm$ from the location of the plasma/airflow/fuel injection interaction region (this is not visible in the schlieren images). As the fuel injection flow rate is increased, the flame front moves forward and gradually occupies the entire combustor downstream from the injector location. Operating at a fuel mass flow rate above $G_{C_2H_4} \approx 6 g/s$ may lead to thermal choking in this combustor geometry. Increasing the duct expansion angle may resolve this problem

Data on TDLAS measurements

The DLAS measurements were performed in typical operation modes : $M=2$, $P_{st}=150 Torr$; the plasma power was $W_{pl}=10-16 kW$, the ethylene mass flow rate was “optimal” for each operation scheme: $G_{C_2H_4}=1.3-1.6 g/s$ for Scheme N°. 1, $G_{C_2H_4}=1.8-2.1 g/s$ for Scheme N°. 2 and $G_{C_2H_4}=2-2.5 g/s$ for Scheme N°. 3. The data on the Z-distribution (cross-flow) of the gas temperature in one of the cross-sections $x=130 mm$ are shown in figure 9. The spectral interval of a single diode laser (DL) scan was about $0.9 cm^{-1}$. Four absorption lines fall within the interval. Depending on the temperature of the probing zone, the relative intensities of the lines vary significantly. The algorithm for the data processing and evolving the parameters of the probed gas flow are described in a previous publication [27]. Each point in the figure was obtained during an individual run of the facility. The values of the temperature inferred from both slopes coincide reasonably well. The accuracy of the measurements could be estimated at $\Delta T = \pm 30K$. Note, the measured temperature is line-averaged on the DL beam pass from wall to wall. In the case of a non-homogeneous distribution of the gas parameters in the reacting zone, a contribution of each individual area is weighted in accordance with the water vapor concentration. This turns the estimation of the maximal gas temperature values into a non-trivial problem.

The result of the measurements indicates a substantial difference in a maximal temperature value and a hot zone thickness depending on the plasma-flow-fuel interaction scheme applied. In the case of upstream plasma generation, the reaction zone is thin compared to that in Schemes N°. 2 and N°. 3. The maximal value of the Y-averaged gas temperature has been observed to be also much lower in this case. The distribution patterns are different as well. Scheme N°. 3, where plasma collocates with the fuel injection jet, demonstrates the highest gas temperature amplitude and a rather thick hot zone in the Y direction. A qualitatively similar result was obtained for a water vapor concentration distribution measured by TDLAS.

Averaged temperature, K

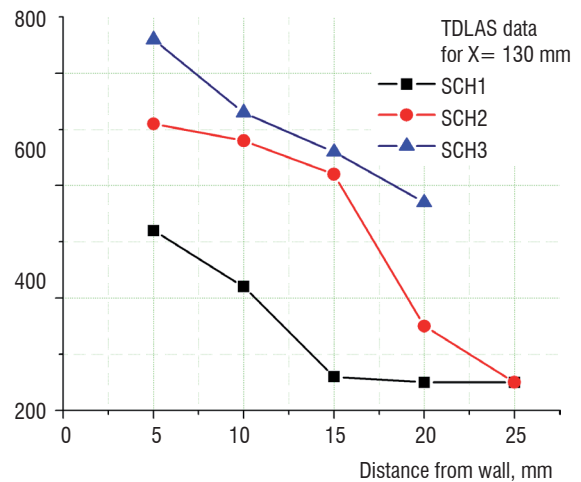


Figure 9 - Temperature of the water vapor distribution cross-flow, measured by TDLAS in a cross-section at $x=130 mm$ from the point of fuel injection. Comparison of the three schemes.

Discussion

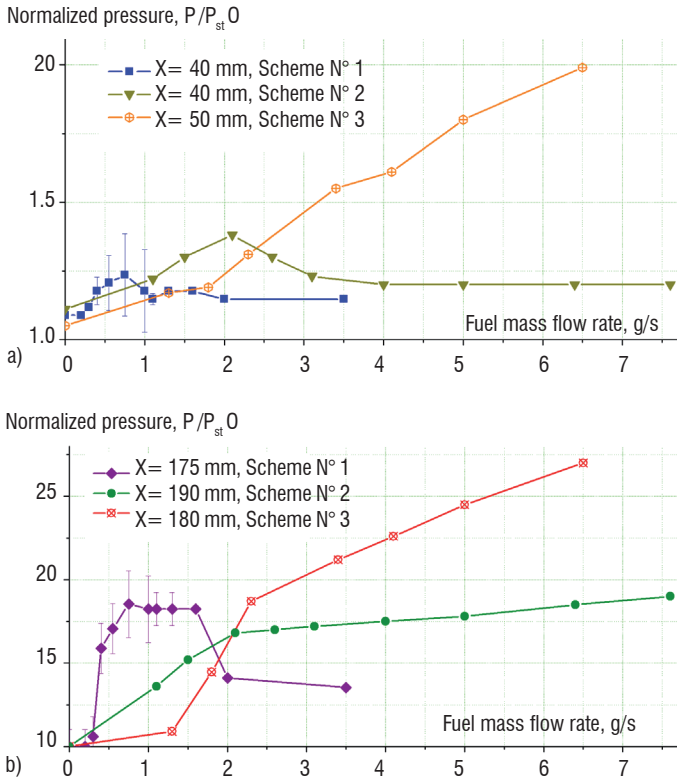


Figure 10 - Comparison of the pressure data depending on the fuel mass flow rate, obtained for the configuration with discharge generation upstream from the fuel injector, downstream from the fuel injector and for a collocated scheme. The flow parameters ($M=2$, $P_{st}=150-200\text{ Torr}$) and discharge power ($W_{pl}=12-18\text{ kW}$) are similar in all cases; the axial location X is measured from the fuel injection cross-section. (a) location of the measuring points in proximity of the fuel injector $x=40-50\text{ mm}$; (b) in the downstream zone $x=175-190\text{ mm}$.

Figure 10 shows a striking difference between the performance of the three schemes applied for plasma-based ignition and flameholding: the previously used schemes with plasma generation upstream [12] and downstream from the fuel injection port [16] and the last scheme with collocated plasma generation and fuel injection, combined into a single unit [24]. The Scheme N° 1 exhibits a more effective ignition under fuel-lean conditions, i.e., at low fuel flow rates. However, the last configuration, Scheme N° 3, shows a much better performance under fuel-rich conditions, where Scheme N° 1 is limited to partial oxidation with a fairly insignificant increase in the pressure. The lean combustion limit for the last configuration is $G_{C_{2H_4}} > 1\text{ g/s}$, while for the previous Scheme N° 1 it was $G_{C_{2H_4}} < 0.4\text{ g/s}$.

In the last experiments with Scheme N° 3, increasing the ethylene flow rate results in a more pronounced pressure rise (i.e., in more intense combustion), which was not the case for the previously tested Configuration N° 1. To interpret this difference, two key points need to be made: (1) in Scheme N° 1, the discharge was sustained in air, while in this scheme it is sustained in the fuel (inside the injection orifice), as well as in the fuel-air mixture; and (2) the flow structure in this Configuration N° 3 is significantly different. Specifically, the near-surface quasi-DC discharge used in Scheme N° 1 produces a “closed” flow separation zone (a separation bubble) downstream

from the discharge, with high concentrations of chemically active species, such as atomic oxygen (O) and electronically/vibrationally excited nitrogen (N_2^*). The fuel, after being injected into this zone, has a sufficiently long residence time to mix with plasma-activated air and ignite. After ignition, the volume of this zone increases and forms an extended subsonic flow zone without obvious reattachment downstream. A further increase in the fuel mass flow rate results in extremely fuel-rich conditions in the separation zone, with subsequent flame extinction/blow-off. Under these conditions, the residual pressure increase indicates a partial oxidation of fuel by active species generated by the discharge. In contrast to this pattern, in Scheme N° 3 the discharge is localized along the fuel injection jet, which generates reactive species and radicals, such as H , CH , C_2H_3 , etc..., by electron impact and enhances mixing by convecting the unstable plasma filament with the injection jet. Based on these results, it appears that filament convection with the flow becomes significant only at a sufficiently high fuel injection speed, comparable with the main airflow velocity. This explains why ignition is not observed under fuel-lean conditions (see figure 10).

Conclusions

The paper discusses the experimental results on plasma-assisted supersonic combustion and flameholding recently obtained at the high-speed combustion facility PWT-50H, using flush-mounted discharge modules. The use of this method may potentially lead to a reduction in the total pressure losses when operating the combustor under non-optimal conditions, enhancement of operation stability and, consequently, the expansion of the air-breathing corridor of the scramjet operation range. The concept of plasma-assisted combustion includes not only accelerating ignition, but also mixing enhancement when operating under non-premixed conditions and flame stabilization (flameholding). This paper presents experimental results showing a significant performance enhancement based on plasma-flow interaction physical mechanisms, which were not understood previously.

The comparison of previously used schemes with the upstream and downstream generation of plasma in relation to the place of fuel injection and the novel scheme of a combined electric discharge/fuel injection module, with the high-voltage electrode placed inside the fuel injection orifice, is depicted in this work. In the last scheme, referred to as Scheme N° 3, after breakdown is achieved, the discharge current path follows the fuel injection jet due to convective entrainment of the plasma by the flow. The axial part of the plasma filament is localized inside the fuel-air mixing layer. The plasma filaments are extended by the fuel injection flow, penetrate into the main airflow and end far downstream, which is critically important for fuel-air mixing acceleration.

Stable flameholding has been observed over a wide range of fuel injection mass flow rates. The critical importance of the plasma module and combustor geometry, as well as that of key operation parameters such as total discharge power, $W_{pl} > 10\text{ kW}$ and fuel mass flow rate $G_{C_{2H_4}} > 1\text{ g/s}$, has been demonstrated. It is also important that these experiments illustrate possible ways for further improvement of this technique, including the use of contoured injector orifices for supersonic injection and a power supply with a modified voltage-current characteristic. Finally, the new scheme demonstrates a significant advantage in terms of flameholding limits, compared to previously tested configurations ■

Acknowledgments

This work was supported by the AFOSR (contract monitor: Dr. Chipping Li) and the AFORL (contract monitor : Dr. Campbell Carter). The authors would like to thank Prof. Igor Adamovich (OSU) and Dr. Vladimir Sabelnikov (ONERA) for multiple discussions and Alec Houpt for his help with the text editing. The authors are grateful to the ISAN team, headed by Prof. Mikhail Bolshov, which performed the TDLAS measurements.

Acronyms

PIM (Plasma-based Injection-Ignition Module)
PWT-50H (Pulse Wind Tunnel of JIHT RAS)
TDLAS (Tunable Diode Laser Absorption Spectroscopy)

References

- [1] E.T. CURRAN - *Scramjet Engines: the First Forty Years*. J. Propul. Power 17 (6), (2001) 1138–1148.
- [2] J. C. B. MACKEAND - *Sparks and Flames: Ignition in Engines : An Historical Approach*. Tyndar Press, 1997.
- [3] A. STARIKOVSKIY, N. ALEKSANDROV - *Plasma-Assisted Ignition and Combustion*. Progress in Energy and Combustion Science, Volume 39, Issue 1, February 2013, Pages 61–110.
- [4] I.V. ADAMOVICH, I. CHOI, N. JIANG, J.-H KIM, S. KESHAV, W.R. LEMPERT, E. MINTUSOV, M. NISHIHARA, M. SAMIMY, and M. UDDI - *Plasma Assisted Ignition and High-Speed Flow Control: Non-Thermal and Thermal Effects*. Plasma Sources Science and Technology, vol. 18, 2009, p. 034018.
- [5] S.M. STARIKOVSKAIA - *Plasma Assisted Ignition and Combustion*. J. Phys.D: Applied Physics, 2006, vol.39, R265-R299.
- [6] M.C. BILLINGSLEY, W.F. O'BRIEN, J.A. SCHETZ - *Plasma Torch Atomizer-Igniter for Supersonic Combustion of Liquid Hydrocarbon Fuels*. AIAA Paper 2006-7970.
- [7] H. DO, M.A. CAPPELLI, M.G. MUNGAL - *Plasma Assisted Cavity Flame Ignition in Supersonic Flows*. Combust. Flame 157 (9) (2010) 1783–1794.
- [8] L.S. JACOBSEN, C.D. CARTER, T.A. JACKSON, et al. - *Plasma-Assisted Ignition in Scramjets*. J. Propul. Power 24 (4) (2008) 641–654.
- [9] K. TAKITA, K. SHISHIDO, K. KURUMADA - *Ignition in a Supersonic Flow by a Plasma Jet of Mixed Feedstock Including CH₄*. Proc. Combust. Inst. 33 (2) (2011) 2383–2389.
- [10] FEI LI, XI-LONG YUA, YING-GANG TONG, YAN SHEN, JIAN CHEN, LI-HONG CHEN, XIN-YU CHANG - *Plasma-Assisted Ignition for a Kerosene Fueled Scramjet at Mach 1.8*. Aerospace Science and Technology 28 (2013) 72–78.
- [11] S. LEONOV, D. YARANTSEV, V. SABELNIKOV - *Electrically Driven Combustion near the Plane Wall in a Supersonic Duct*. Progress in Propulsion Physics, Advances in Aerospace Science, EUCASS book series, Vol 2, 2011, pp. 519-530.
- [12] S. LEONOV, C. CARTER, D. YARANTSEV - *Experiments on Electrically Controlled Flameholding on a Plane Wall in Supersonic Airflow*. Journal of Propulsion and Power, 2009, vol.25, N°2, pp.289-298.
- [13] Z. YIN, I.V. ADAMOVICH, and W.R. LEMPERT - *OH Radical and Temperature Measurements During Ignition of H₂-Air Mixtures Excited by a Repetitively Pulsed Nanosecond Discharge*. Proceedings of the Combustion Institute, vol. 34, 2013, pp. 3249–3258.
- [14] W. SUN, M. UDDI, T. OMBRELLO, S.H. WON, C. CARTER, Y. JU - *Effects of Non-Equilibrium Plasma Discharge on Counterflow Diffusion Flame Extinction*. Proceedings of the Combustion Institute 33 (2), 3211-3218, 2011.
- [15] I. N. KOSAREV, V. I. KHORUNZHENKO, E. I. MINTOUSOV, P. N. SAGULENKO, N. A. POPOV, S. M. STARIKOVSKAIA - *A Nanosecond Surface Dielectric Barrier Discharge at Elevated Pressures: Time-Resolved Electric Field and Efficiency of Initiation of Combustion*. Plasma Sources Science & Technology, vol. 21, N° 4, 2012.
- [16] A. FIRSOV, S. LEONOV, D. YARANTSEV et al - *Temperature Measurement in Plasma-Assisted Combustor by TDLAS*. Paper AIAA 2012-3181.
- [17] S. B. LEONOV, A. A. FIRSOV, YU. I. ISAENKOV et al. - *Plasma-Based Fast Mixing and Ignition in Supersonic Flow*. Paper AIAA 2011-2327.
- [18] S. B. LEONOV AND D. A. YARANTSEV - *Near-Surface Electrical Discharge in Supersonic Airflow: Properties and Flow Control*. Journal of Propulsion and Power, vol. 24, 2008, pp. 1168-1181.
- [19] C. O. LAUX, T. G. SPENCE, C. H. KRUGER and R. N. ZARE - *Optical Diagnostics of Atmospheric Pressure Air Plasmas*. Plasma Sources Sci. Technol. 12 (2003) 125–138.
- [20] M. A. GIGOSOSY and V. CARDENOSOZ - *New Plasma Diagnosis Tables of Hydrogen Stark Broadening Including Ion Dynamics*. J. Phys. B: At. Mol. Opt. Phys. 29 (1996) 4795–4838.
- [21] H. R. GRIEM - *Stark Broadening of the Hydrogen Balmer- α Line in Low and High Density Plasmas*. Contrib. Plasma Phys. 40 (2000), pp.46-56.
- [22] A. A. FIRSOV, M. A. SHURUPOV, D. A. YARANTSEV, S. B. LEONOV - *Plasma-Assisted Combustion in Supersonic Airflow : Optimization of Electrical Discharge Geometry*. Paper AIAA-2014-0988.
- [23] C.S. KALRA, S.H. ZAIDI, R.B. MILES, and S.O. MACHERET - *Shockwave–Turbulent Boundary Layer Interaction Control Using Magnetically Driven Surface Discharges*. Experiments in Fluids, vol. 50, 2011, pp. 547–559.
- [24] K.V. SAVELKIN, D.A. YARANTSEV, I.V. ADAMOVICH, and S.B. LEONOV - *Ignition and Flameholding in a Supersonic Combustor by an Electrical Discharge Combined with a Fuel Injector*. Published online in Combustion and Flame, 2014, <http://dx.doi.org/10.1016/j.combustflame.2014.08.012>.
- [25] M. A. DEMINSKY, I. V. KOCHETOV, A. P. NAPARTOVICH, S. B. LEONOV - *Modeling of Plasma Assisted Combustion in Premixed Supersonic Gas Flow*. International Journal of Hypersonics, Volume 1, N° 4, December 2010, pp. 5-15.
- [26] A. A. ZHELTOVODOV and E. A. PIMONOV - *Using a Localized Pulse Periodic Energy Supply for Intensification of Mixing of Parallel Compressible Flows*. Technical Physics Letters, 2013, Vol. 39, N° 11, pp. 1016–1018.
- [27] M. A. BOLSHOV, Y. A. KURITSYN, V. V. LIGER, V. R. MIRONENKO, S. B. LEONOV, D. A. YARANTSEV - *Measurements of the Temperature and Water Vapor Concentration in a Hot Zone by Tunable Diode Laser Absorption Spectrometry*. Appl. Phys. B Lasers and Optics (2010), v.100, N° 2, 397-407.



Konstantin Savelkin graduated from Moscow Aviation Institute with a degree in radioelectronics equipment in 1986. Now he works as leading engineer in Joint Institute for High Temperatures Russian Academy of Science, Department of Plasma Aerodynamics and Combustion Control. He designs and assembles the power sources for different types of plasma generators as well as maintains wind tunnel experimental facility.



Dmitry Yarantsev graduated from Moscow Power Engineering Institute (Technical University) with a master degree in nuclear power plants and thermonuclear facilities in 2001. Now he works as research scientist in Joint Institute for High Temperatures Russian Academy of Science, Department of Plasma Aerodynamics and Combustion Control. He develops diagnostic techniques and performs experimental research in the field of plasma assisted combustion in high speed flow and flow control by plasma.



Sergey B. Leonov works as a Research Professor in University of Notre Dame, USA, Aerospace and Mechanical Engineering Department. He graduated from the Moscow State University, 1981, and received PhD degree in mechanics of gases and plasma from the Baltic State University, in 1991. In 2006 he has got the degree of Doctor of Science in physics and mathematics. Since 1998 he is Head of Laboratory and since 2009 is Head of Department in the Joint Institute for High Temperature Russian Academy of Sciences. Since 2009 he is a Professor in Moscow Open University. In 2013-2014 he is a Visiting Professor in The Ohio State University, USA, Mechanical and Aerospace Engineering Department. The main subjects of his interest are experimental plasma aerodynamics, plasma assisted combustion, plasma diagnostics, gasdynamics and aerodynamics, weakly ionized plasma generation.